CHARACTERISTICS OF THE SPACE–TIME EVOLUTION OF VAPOR–GAS CAVITIES GENERATED BY AN UNDERWATER SPARK DISCHARGE

A. I. Vovchenko, V. V. Kucherenko, and V. V. Shamko

UDC 532.528

Once the electrical energy of a charged capacitor has been completely released in the elements of the discharge circuit the spark channel converts into a vapor–gas cavity (VGC), which executes a series of successive pulsations. The latter are accompanied by acoustic emission and the formation of nonsteady hydrodynamic streaming, which comprises the principal driving factor in the electrohydrodynamic percussion treatment of materials [1]. In addition to the nonsteady motion of the VGC, the mass and composition of the gas in it vary with time. Consequently, the description of effects of this kind poses one of the most difficult problems in the mechanics of liquids, gases, and plasma.

For the calculation of the acoustic emission and nonsteady hydrodynamic streaming it is important to know the law of motion of the boundary of the VGC [2, 3], and for the estimation of the force parameters it is equally important to understand its extremal space–time characteristics [2-4].

A mathematical model of the effect has been developed only for spherical [5] and cylindrical [6-9] cavities. In regard to the dynamics of cavities of other configurations [1, 3, 10-12], so far the only available information has been accumulated mainly on the basis of experimental studies. On the other hand, data on the extremal space–time characteristics of VGCs other than a sphere as a function of the electrical-engineering parameters of the discharge are practically nonexistent in the literature.

In the present study we investigate the space–time evolution of cavities of various geometries generated by an underwater spark discharge (USD) for the purpose of determining the correlation of the fundamental extremal kinematic characteristics with the initial parameters of the energy source. We have solved the stated problem experimentally, making use of high-speed motion-picture techniques.

The experiments were carried out in a special tank (1500 × 1000 × 500 mm) filled with distilled water and equipped with two Plexiglas illuminators, which enabled us to photograph the process in transmitted light rays from a high intensity source. The discharge was maintained stable (along with the cavity parameters) as a result of rectification of the spark channel by means of a Constantan initiating microconductor (3 μm in diameter) and natural degassing of the liquid. The discharge was fired at a depth of 0.24 m, and copper needles 4 mm in diameter were used for the electrodes.

Vapor–gas cavities of various geometries were generated according to the discharge regime; see Fig. 1: a) spherical ($W_\tau/l > 1$ kJ·m^{-1}); b) ellipsoidal ($0.1 \leqslant W_\tau/l \leqslant 1$ kJ·m^{-1}); c) cylindrical ($W_\tau/l < 0.1$ kJ·m^{-1}). Here W_τ is the energy released in the USD channel, and l is the length of the discharge channel. The time between frames is as follows: a) 0.185; b) 0.172; c) 0.181 msec. It is seen that the spherical and cylindrical cavities retain their symmetry until they attain their minimum size, whereas the shape of the ellipsoidal VGCs changes with time.

A particular collapse pattern is realized by the VGC, depending on its geometry (see Fig. 1), and the coefficient of energy utilization of the hydrodynamic pressure–velocity field in the electrohydrodynamic percussion treatment of materials varies accordingly [1].

Experience has shown [13] that the main fraction (up to 95%) of the cavity energy W is spent in the first expansion–compression cycle; in subsequent pulsations the VGC no longer has a distinct geometrical shape. The ensuing analysis is therefore aimed exclusively at this important practical phase of the motion.

Nikolaev. Translated from Zhurnal Prikladnoi Mekhaniki i Tekhnicheskoi Fiziki, No. 6, pp. 58-64, November-December, 1978. Original article submitted October 31, 1977.

0021-8944/78/1906-0755$07.50

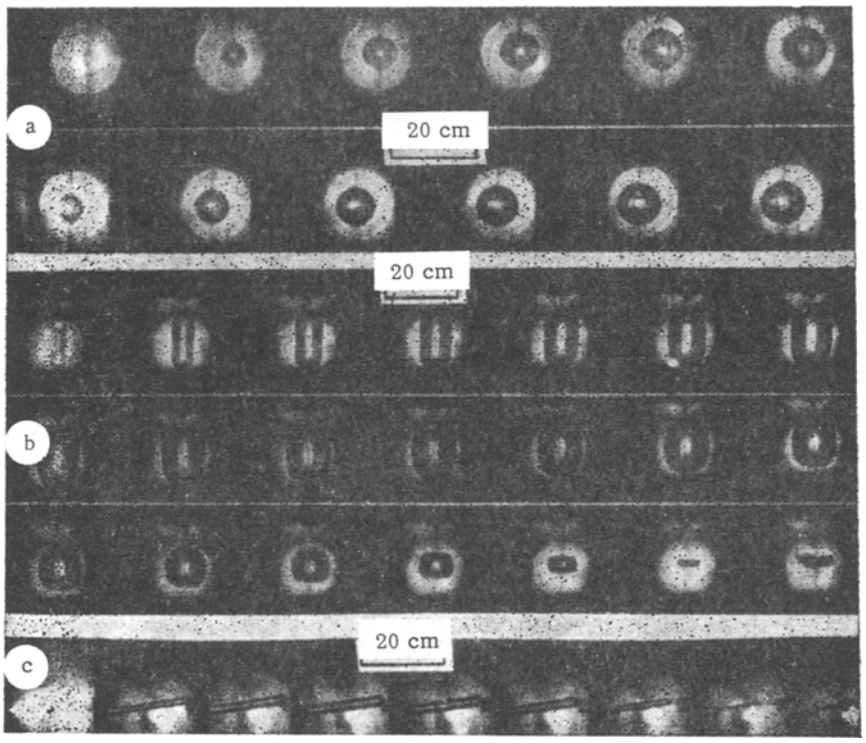

Fig. 1

A good general characteristic of the ellipsoidal and cylindrical cavities is the compression ratio, defined here as the ratio of the meridian diameter to the equatorial diameter, k = D/d. The time ($\bar{t}$ = t/T) variation of the compression ratio during the first pulsation of the VGC is shown in Fig. 2: 1) $W_\tau l^{-1}$ = 12 kJ•m^{-1}, τ = 1.4 μsec; 2) 0.1, 23; 3) 0.19, 2; 4) 3.6, 18; 5) 6.1, 15; 6) 6.1, 46. Curve 4 corresponds to the pulsation of a cylindrical cavity between two flat solid walls perpendicular to its symmetry axis. It is evident from Fig. 2 that if $(D/d)_{max} > 2$ at the maximum cavity size it remains prolate (k > 1) during the entire pulsation period; in energy units this condition corresponds to the inequality $W_\tau/l < 1$ kJ•m^{-1}; here we have the generalized dependence of the cavity pulsation period on its compression ratio at the instant of maximum volume. The interval $1 < k_{max} \leqslant 5$ corresponds to the collapse of ellipsoidal cavities, the period of whose first pulsation is described by an empirical relation of the form

$$T = 1.83 a_{max} \sqrt{\rho_0/p_0}\, k_{max}^{1/3}, \tag{1}$$

from which follows, for k_{max} = 1, the Willis equation [3].

An analysis of the experimental data shows that at the instant when an ellipsoidal cavity attains maximum volume the meridian diameter is roughly twice the interelectrode gap. As a result, the function $T(a_{max})$ for ellipsoidal VGCs can be written in the form

$$T = 1.83 l^{1/3} a_{max}^{2/3} \sqrt{\rho_0/p_0}. \tag{2}$$

In the given case the linear relationship that exists between the indicated extremal quantities for spherical cavities is violated. It is interesting to note that linearity is preserved if the maximum linear scale is interpreted as the equivalent radius $\langle a \rangle$ of a sphere of equal volume:

$$T \simeq 1.6 \langle a \rangle \sqrt{\rho_0/p_0}.$$

Beginning with $k_{max} > 5$, collapse of the VGC corresponds to the cylindrical model, and the following expression is valid for its pulsation period in accordance with Fig. 2:

$$T = 3.3 a_{max} \sqrt{\rho_0/p_0}, \tag{3}$$

which differs from Kedrinskii's expression [6] only by a numerical factor. The latter is clearly atrributable to the boundedness of the liquid volume in the experiment.

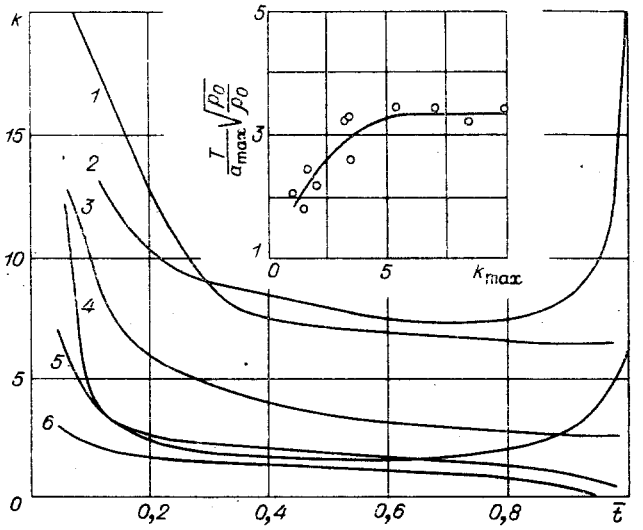

Fig. 2

To determine the relationship between the maximum radius and the parameters of the energy source we also make use of the experimental data of [10], which mirror the fact of the governing dependence of the energy fraction of the VGC η_1 on the cavity form factor $\beta = l^{-1}(W_\tau p_0^{-1})^{1/3}$ and the very weak dependence on the rate of energy release. The use of the parameter β in determining a_{max} makes it possible, by contrast with [4, 14], to take the discharge regime into account. The approximation of the tabulated values of $\eta_1(\beta)$ (see Table 1.1 of [10] as well as the columns 3 and 4 in our Table 1) yields a relation of the type

$$\eta_1 = 0.26 \exp(-2/3 \cdot \beta) + 0.14. \tag{4}$$

It is seen that as the shape of the cavity approaches spherical ($\beta \to 0$) the fraction η_1 increases, tending to a value of 0.4, and as it approaches cylindrical ($\beta \to \infty$) the fraction decreases, arriving in the limit at $\eta_1 = 0.14$. The decrease of η_1 with elongation of the VGC is attributable to the increase in the energy losses of the cavity due to emission and heat conduction as its surface area grows for a fixed volume.

Knowing that the VGC energy is determined, on the one hand, by the maximum volume V_{max} ($W = p_0 V_{max}$) and, on the other, by W_τ ($W = \eta_1 W_\tau$), for the maximum radius of spherical, ellipsoidal, and cylindrical cavities, in accordance with (1)-(4), we write a simple equation of the type

$$a_{max} = \alpha \left[0.26 \exp\left(-\frac{2}{3} \frac{l p_0^{1/3}}{W_\tau^{1/3}} \right) + 0.14 \right]^{\lambda}. \tag{5}$$

Here α and λ are parameters depending on the VGC geometry:

$$\text{sphere: } \alpha = \left(\frac{3}{4\pi} \frac{W_\tau}{p_0} \right)^{1/3}, \quad \lambda = \frac{1}{3};$$

$$\text{ellipsoid: } \alpha = \left(\frac{3}{4\pi} \frac{W_\tau}{l p_0} \right)^{1/2}, \quad \lambda = \frac{1}{2};$$

$$\text{cylinder: } \alpha = \left(\frac{W_\tau}{\pi l p_0} \right)^{1/2}, \quad \lambda = \frac{1}{2}.$$

The energy released in a medium-power discharge channel* with characteristic time constant $\pi\sqrt{LC} \leqslant 40$ μsec is determined in the first approximation according to the procedure of [15] on the basis of the amplitude and frequency parameters obtained in [16], as follows. Since the resistance R(t) of the spark channel varies considerably less in later half-periods of the current oscillations than in the first half-period, in calculating the energy release in the discharge channel we can average R(t) with respect to the time and determine its average value $\bar{R}$ from the decay of the discharge current:

$$\bar{R} = \frac{2L}{T_i} \ln \frac{i_m}{i_{m-1}} - R_0,$$

*By medium-power discharges we conditionally mean discharges that obey an inequality of the type $W_\tau l^{-1} < 10^5$ J·m^{-1}.

where T_i is the period of the current oscillations, C and L are the capacitance and inductanc of the circuit, and R_0 is the equivalent resistance of the elements of the discharge circuit for $l = 0$.

Then with the discharge current i(t) approximated by a damped sine function $i(t) = U_b \sqrt{C/L}\, e^{-\delta t} \sin \omega t$ the value of the energy released in the channel at any instant can be determined from the expression

$$W(t) = W_1(t)\,\sigma_0(t)\,\sigma_0(\tau_1 - t) + \frac{I_1^2 \bar{R}}{4\delta}\left\{\frac{\omega^2}{\delta^2+\omega^2}\, e^{-2\delta\tau_1} - \right.$$
$$\left. - e^{-2\delta t}\left[1 + \frac{\delta^2}{\delta^2+\omega^2}\left(\frac{\omega}{\delta}\sin 2\omega t - \cos 2\omega t\right)\right]\sigma_0(t-\tau_1)\right\}. \quad (6)$$

Here $W_1(t)$ denotes the instantaneous values of the energy released in the first half-period of the current oscillations, $\omega = (LC)^{-1/2}$, $\delta = (R_0 + \bar{R})/2L$, $\eta = [\pi(Al^2/U_b^2\sqrt{LC})]^{1/3}$, $\tau_1 = (1 + 0.65\eta^2)\pi\sqrt{LC}$ is the duration of the first current half-period, A is the spark constant [16], $\sigma_0(t-\tau_1) = \begin{cases} 0, & t < \tau_1 \\ 1, & t \geqslant \tau_1 \end{cases}$ is the unit Heaviside function, U_b is the breakdown voltage of the water gap,

$$I_1 = \left[(1-\eta)\frac{CU_0^2}{L} - 0.05\pi(1+0.65\eta^2)\, i_1^2\right]^{1/2},$$

and U_0 is the charging voltage of the capacitor bank.

For $\bar{R}$ we have an empirical equation [15] of the type

$$\bar{R} \simeq 0.15\eta(1 + 5\eta^3)\sqrt{L/C}. \quad (7)$$

By generalizing the experimental data ([13], see Fig. 3) for $R_0 \approx (0.03\text{-}0.1)\sqrt{L/C}$ we obtain the last unknown parameter — the current amplitude in the first half-period:

$$i_1 = U_b\sqrt{C/L}(1 - 0.65\eta^2). \quad (8)$$

As a result, the energy released in the discharge channel can be determined from the expression

$$W_\tau \approx \eta\frac{CU_b^2}{2} + \frac{I_1^2\bar{R}\omega^2}{4\delta(\omega^2+\delta^2)}\left(e^{-2\delta\tau_1} - e^{-2\delta\tau}\right), \quad (9)$$

in which

$$\tau = \pi\sqrt{LC}(11.7\eta^2 - 24.2\eta + 14.3). \quad (10)$$

The energy-release law (6) obtained above is also valid for powerful ($W_\tau l^{-1} > 10^5$ J·m^{-1}) USDs with a time constant $\pi\sqrt{LC} > 40$ μsec. For such discharges we have obtained the following approximate electrical relations on the basis of a generalization of the experimental data of [13]:

fraction of the total energy released in the first half-period,

$$\eta = 1.05 + 0.36\lg\frac{bl^2}{U_b^2\sqrt{LC}}; \quad (11)$$

equivalent spark resistance for $t \geqslant \tau_1$,

$$\bar{R} \simeq 0.35\eta(1 + 2\eta^3)\sqrt{L/C}; \quad (12)$$

duration of first half-period of the discharge current,

$$\tau_1 = \pi\sqrt{LC}(1 - 0.33\eta^4)^{-1}; \quad (13)$$

first current amplitude,

$$i_1 = U_b\sqrt{C/L}\, e^{-0.5\eta^3}(1+\eta^2)^{-1}(1 + \eta e^{-0.78/\eta}), \quad (14)$$

all as a function of the energy source parameters in the interval $0.3 \leqslant \eta \leqslant 0.9$ ($b = 10^5$ V^2·sec·m^{-2}).

Table 1 compares the maximum radii calculated for spherical, ellipsoidal, and cylindrical cavities generated by an USD according to expressions (5)-(14) with the experimental results of the present study and [17, 18].

TABLE 1.

No.	W_τ/l, kJ/m^{-1}	β	η_1, %	a_{max}, m	
				calc.	exp.
1	772,0	4,6	19,4	0,57	0,41
2	280,0	12,5	50,5	0,21	0,23
3*	81,6	6,12	51,3	0,16	0,18
4*	36,7	4,8	40,0	0,12	0,13
5†	19,3	19,8	33	0,046	0,042
6†	13,9	17,7	33	0,040	0,033
7	1,3	2,1	27,7	0,100	0,092
8	0,1	0,43	23,6	0,007	0,008

*Data of [17].
†Data of [18].

The maximum discrepancy between the calculated and experimental data is 13% for medium-power discharges and 35% for powerful discharges. Thus, the proposed method of analysis of nonsteady pulsations of cavities generated by underwater spark discharges of various powers and thereby invested with different geometrical configurations makes it possible to determine the extremal parameters of the cavities without resorting to experiment and, accordingly, to find their force characteristics.

LITERATURE CITED

1. V. V. Shamko and A. I. Vovchenko, "Influence of the boundary surfaces on the evolution of a vapor–gas cavity associated with an underwater spark discharge," in: Fluid Mechanics [in Russian], No. 34, Naukova Dumka, Kiev (1976).
2. I. Ya. Miniovich, A. D. Pernik, and V. S. Petrovskii, Hydrodynamic Sound Sources [in Russian], Sudostroenie, Leningrad (1972).
3. K. A. Naugol'nykh and N. A. Roi, Electrical Discharges in Water [in Russian], Nauka, Moscow (1971).
4. L. L. Telyashov, V. A. Okhitin, and A. G. Polvik, "Experimental investigation of the collapse phase of a vapor–gas cavity in water," in: Proceedings of the Symposium on the Physics of Acoustohydrodynamic Phenomena [in Russian], Nauka, Moscow (1975).
5. R. H. Cole, Underwater Explosions, Princeton University Press, Princeton, New Jersey (1948).
6. V. K. Kedrinskii, "Pulsation of a cylindrical gas cavity in an unbounded liquid," in: Continuum Dynamics [in Russian], No. 8, Izd. Inst. Gidrodinam., Novosibirsk (1971).
7. V. K. Kedrinskii, "Approximative models of the one-dimensional pulsation of a cylindrical cavity in an incompressible liquid," Fiz. Goreniya Vzryva, No. 5, 768-773 (1976).
8. V. K. Kedrinskii and V. G. Kuzavov, "Dynamics of a cylindrical cavity in a compressible liquid," Zh. Prikl. Mekh. Tekh. Fiz., No. 4, 102-106 (1977).
9. A. N. Salov, "Interaction of gas bubbles in the time-spaced detonation of elongated charges in a liquid of finite depth," Tr. Novosibirsk. Inst. Inzh. Vodnogo Transporta, No. 101, 29-40 (1975).
10. I. Z. Okun' and B. S. Fraiman, "Energy of a gas bubble generated by a pulse discharge in water," Izv. Vyssh. Uchebn. Zaved., Fiz., No. 8, 154-157 (1969).
11. R. T. Knapp, J. W. Daily, and F. G. Hammitt, Cavitation, McGraw-Hill, New York (1970).
12. V. A. Burtsev and V. V. Shamko, "Collapse of a spherical cavity induced by an underwater spark near a solid wall," Zh. Prikl. Mekh. Tekh. Fiz., No. 1, 80-90 (1977).
13. Investigation of the Dynamics of Evolution of Powerful Electrical Discharges in Water with Peak Discharge Current up to 400 kA [in Russian], Rep. B 556838, PKB Élektrogidravliki Akad. Nauk UkrSSR, Nikolaev (1976).
14. Yu. E. Sharin and V. A. Korotkov, "Investigation of the electrical efficiency and energy of pulsation of a gas cavity associated with pulse discharge in water," in: High-Temperature Heat Physics [in Russian], Nauka, Moscow (1969).
15. I. Z. Okun', "Investigation of the electrical characteristics of a pulse discharge in a liquid," Zh. Tekh. Fiz., 39, No. 5, 837-861 (1969).

16. V. V. Shamko and E. V. Krivitskii, "Investigation of certain characteristics of an underwater spark channel in the main stage of evolution of discharge," Zh. Tekh. Fiz., 47, No. 1, 93-101 (1977).
17. G. S. Lursmanashvili, "Energy of a gas bubble, shock wave, and light radiation," in: New Research in Mining [in Russian], No. 3, Izd. Leningr. Gorn. Inst., Leningrad (1971).
18. A. G. Ryabinin and G. A. Ryabinin, "Experimental study of the energy of a gas bubble associated with electrical discharge in water," Zh. Tekh. Fiz., 46, No. 4, 881-884 (1976).

MOTION OF A SPHERE IN AN INFINITE CONDUCTIVE FLUID, PRODUCED BY A VARIABLE MAGNETIC DIPOLE LOCATED WITHIN THE SPHERE

V. I. Khonichev and V. I. Yakovlev

UDC 538.4

§1. In [1] a study was made of two examples of turbulent flow developing in a conductive fluid under the action of an ac magnetic field. In one of these the electromagnetic field was created by a magnetic dipole $\mathbf{m}_0 e^{i\omega t}$ located in the center of a nonconductive solid sphere immersed in an infinite volume of conductive fluid. Due to the high degree of symmetry the applied electromagnetic field did not lead to directed motion of the fluid relative to the sphere.

It is of interest to consider the case of a less symmetric electromagnetic field in which the net force exerted on the fluid by the field is nonzero. Such a situation should lead to the development of a translational component in the fluid motion relative to the solid body or, what is the same, to translational motion of the solid relative to the fluid, which is at rest at infinity.

For this purpose the present study will consider the flow about a sphere, with the ac dipole displaced relative to the center of the sphere (Fig. 1).

The problem will be solved with the assumption that the eccentricity d is small in comparison to the sphere radius a,

$$\varepsilon = d/a \ll 1, \tag{1.1}$$

and that the conventional and magnetic Reynolds numbers are also small,

$$\mathrm{Re} = v_0 a/\nu \ll 1; \tag{1.2}$$

$$\mathrm{Re}_m = 4\pi\sigma v_0 a/c^2 \ll 1, \tag{1.3}$$

where v_0 is the characteristic velocity of the flow which develops and σ and ν are the conductivity and kinematic viscosity of the liquid. It should be noted that, in fact, condition (1.3) follows from Eq. (1.2), since for all conductive fluids $\nu_m = c^2/4\pi\sigma \gg \nu$.

We will consider the flow which is established after the system achieves a periodic regime.

For the case of constant electric and magnetic fields the first step in the investigation of sphere motion was made in [2], where the force of electromagnetic origin tending to set the sphere in motion relative to the conductive fluid was found (the hydrodynamic portion of the problem was not considered, although estimates were made of the effectiveness of such a means of locomotion in seawater).

§2. In view of assumption (1.3), the fluid motion exerts no effect on the electrodynamic quantities, so that the problem of defining **E** and **H** over all space is separate from the hydrodynamic problem.

The desired fields **E** and **H** are defined by a vector potential **A**: $\mathbf{E} = -(1/c)\partial\mathbf{A}/\partial t$, $\mathbf{H} = \mathrm{rot}\,\mathbf{A}$ where in the spherical coordinate system (r, θ, α) affixed to the sphere the vector **A** has one (nonzero) component $\mathbf{A} = A(r, \theta, t)\mathbf{e}_\alpha$. Since the displacement d of the center of the

Novosibirsk. Translated from Zhurnal Prikladnoi Mekhaniki i Tekhnicheskoi Fiziki, No. 6, pp. 64-71, November-December, 1978. Original article submitted November 22, 1977.

 0021-8944/78/1906-0760$07.50